

Design and Performance Evaluation of a Dry Grain Microniser

Oriaku E. C¹, Agulanna C. N¹, Odenigbo J. O¹, Aburu C. M², Ibeagha D. C¹,
and Adizue U. L¹

¹Engineering Research Development and Production (ERDP) Department.

Projects Development Institute, (PRODA) Emene, Enugu.

²Scientific Equipment Development Institute (SEDI) Enugu.

Corresponding Author: Oriaku E. C

ABSTRACT: The need to add value to agro produce in order to convert them to storable end products is of great importance to the economic growth of any nation. Conversion of dry grains and allied dry products to flour (particles ranging from 5 -50 microns) is indeed example of the value addition. In view of this a dry grain micronizing machine was designed, fabricated and tested under different angular speeds. Dry toasted soya bean seeds of moisture content 9.05%db were used for the test. The speeds ranged from 1500 – 3750 rpm. 2kg of sample was crushed completely in each 4 minutes run of the machine and the dust collected through a cyclone. Particles collected were analysed using an Ocular micrometer and the results tabulated. Graphs of particle ranges with frequency were plotted against percentage collection. The results showed that speeds between 1500 – 2250 rpm produced coarse particle while 2500 – 3750 rpm produced a high percentage of flour particles. Considering the time expended to achieve this it is expected that the machine can handle large quantities of produce per day.

Keywords: Size reduction, micronizer, soya bean, particle size, angular speed.

Date of Submission: 28-04-2018

Date of acceptance: 14-05-2018

I INTRODUCTION

Successfully choosing an appropriate size reduction machine requires an in-depth understanding of the material, the application requirements, and the range of available equipment that can achieve the size reduction goals. It is important to note that the material's hardness and other characteristics affect which size reduction mechanisms are suited to handling the material (Pallmann, 2011). Some of the most common reasons for reducing a material are to create appropriate particle sizes for subsequent processing or end use or create a free-flowing material. Size reduction is also carried out with the aim of improving material blending and preventing segregation by making different sized products with similar particle size distributions. Increasing a material's surface area to improve a material's reactivity (or availability) or drying efficiency is also targeted when reducing size, while controlling a material's bulk density by creating a particle size distribution consisting of a matrix of larger particles with smaller particles filling the voids between the larger particles can be achieved at the same time (Scott et al, 2002). Important properties of the material apart from its size are hardness (measured with the mohr's scale), structure, moisture content, crushing strength, Friability, stickiness and soapiness (Coulson et al, 1978).

The size of the particles affects the properties of a powder or products in many ways (Allen, 1981). Gregory et al (2017), emphasized that the outcome of a grinding operation is the particle size distribution, while the real objective is to control the performance of the final product quality. Ghaid et al (2009) examined the influence of milled grain particle size on the kinetics of enzymatic starch digestion. Two types of cereal (barley and sorghum) were ground and the resulting grounds separated by size using sieving, with ranges of 0.1 to 3.0mm. More so, Marianne et al (2002), proposed that the increased subsample size and particle size reduction are the two factors responsible for subsampling error for explosives residues. Mendardo et al (2012), in his work, four agricultural by products (wheat, barley, rice straw and maize stalk) underwent various mechanical and thermal treatment prior anaerobic digestion including particle size reduction to 5.0, 2.0, 0.5 and 0.2cm and heat application to 90°C and 120°C. Results show that mechanical pre-treatment increased by product methane yield more than 80%.

Therefore it's of great importance to make these particle size reduction machines available in areas of dear need. Thus in this paper a dry grain micronizing machine was designed, fabricated and tested under different angular speed.

II DESCRIPTION AND PRINCIPLE OF OPERATION:-

The side elevation and isometric drawing of the designed micronizer are shown in Appendix I. The micronizer consists of the following components namely:

- | | |
|---------------------------------|--------------------------------------|
| (i) Structural base | (ii) Cylindrical micronizing chamber |
| (iii) Micronizing chamber cover | (iv) Micronizing hexagonal hammers |
| (v) Impeller | (vi) Inlet hopper |
| (vii) Hopper throat | (viii) Impeller guide |
| (ix) Discharge spout | (x) Micron sieve |
| (xi) Impeller shaft | (xii) Suction blower |
| (xiii) Blower impeller | (xiv) Suction channel |
| (xv) Bearing (Plummer block) | (xvi) Multiple stage pulley |
| (xvii) Blower shaft | (xviii) Blower pulley |
| (xix) B- Belts | (xx) Electric motor |
| (xxi) Blower casing | (xxii) Blower discharge channel |
| (xxiii) Fibre gaskets | (xxiv) Bolts and Nuts |

The micronizing chamber houses the impeller which is adapted to the shaft at one end. The shaft is suspended on two deep groove ball bearings. In the same manner, the blower casing houses the blower impeller, which is adapted to the shaft at one end. The shaft is also suspended on two bearings. All the bearings are mounted on the structural frame work. The drive of the machine comes from a robust electric motor. A double groove pulley on one end of the micronizing shaft transmits motion to the blower impeller via a V-belt. All the components of the machine systematically arranged are mounted on a robust structural frame work. The principle of design of this machine is based on the dynamics of the machine components namely pulley, belt, bearing, shaft and hexagonal hammers. Circular motion of these components, combined with the gravitational motion of the items to be crushed and air suction of the crushed items are employed to achieve the desired result. Air flow is employed to remove the micronized powder through the sieve to the cyclone collector.

2.1 Micronizing chamber:

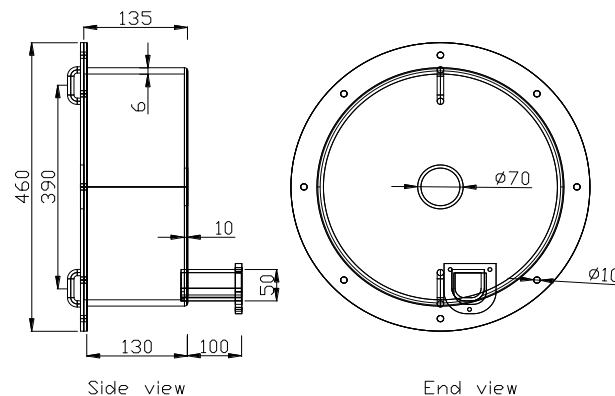


Fig 1: Schematic diagram of micronizing chamber

The Fig above shows the drawing of the micronizing chamber. It is cylindrical with dimensions as follows:

- (a) Diameter of chamber (D_c) = 390 mm = 0.39 m
 Length of micronizing chamber (L_c) = 135 mm = 0.135 m

2.1.1 Volumetric capacity (V_c) of Micronizing Chamber:

$$V_c = \pi r^2 h \quad V_c = 3.142 \times \left(\frac{0.39}{2}\right)^2 \times 0.135$$

$$V_c = 0.042 \text{ m}^3$$

The impeller of the micronizer will rotate in this chamber at a maximum speed of 3750 rpm.

2.1.2 Angular Velocity (ω) of Rotation:

$$\omega = \frac{2\pi N}{60} \qquad \omega = 392.75 \text{ rad/sec}$$

2.1.3 Centrifugal Force (F_c) Developed as a Result of the Rotation:-

$$F_c = m\omega^2 r \qquad F_c = 1122.2\text{N} \qquad (1)$$

Where, m = mass of belt used for the drive
 r = radius of pulley used diameter of pulley = 100mm; $r = 0.05\text{m}$

2.1.4 Mass of Belt (M_b) driving the impeller:

Mass = cross-sectional area of belt x density x belt length:

$$M_b = A_b \times \rho_b \times L_{b1} \qquad (2)$$

$$M_b = 0.1455\text{kg}$$

Note $L_{b1} = 1\text{m}$

2.1.5 Cross Sectional Area of Belt (A_c):

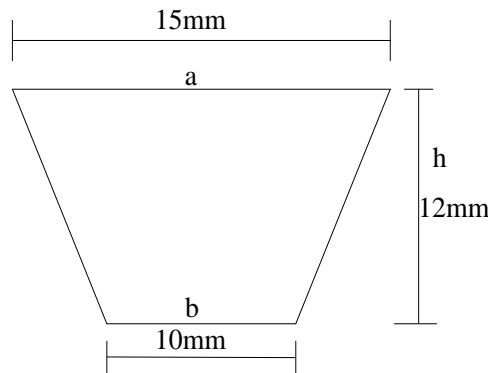


Fig 2: Cross sectional area of belt

The dimension of a section of the belt is shown above. The trapezoidal cross sectional area is thus calculated as

$$A_b = \frac{1}{2}(a + b)h \qquad (3)$$

$$A_b = 0.00015 \text{ m}^2$$

The density (ρ_b) of fabric material (the polythene fibre) of the belt is obtained as

$$\rho_b = 970 \text{ kg/m}^3 \text{ (Chawla, 1998)}$$

• Pressure developed in the micronizing Chamber:

The cylinder is not completely closed at both ends. At one end there exists a hole at the central axis connected to the hopper which is open to the atmosphere. At the other end there exist a rectangular hole on which a micron sieve is mounted which is also open. Through this hole the blower sucks the crushed dust away. It is then clear that the pressure developed in the micronizing chamber should be slightly above atmospheric pressure. Based on this reason an operating pressure of $1.5 \times 10^6 \text{ Nm}^{-2}$ was assumed for this design.

$$P = 1.5 \times 10^6 \text{ Nm}^{-2}$$

From the equation on pressure above $P\pi L(R^2 - r^2) = F_c \qquad (4)$

$$(R^2 - r^2) = \frac{F_c}{P\pi L} \qquad (5)$$

2.2 Micronizing Impeller:

It has two main components namely

- a) The micronizing hexagonal rods and
- b) The circular disc carrying the rods. The rods are thirty (32) in number.

2.2.1 Mass of Impeller (m_i):

$$M_i = \rho_i \times V_T = 28 \text{ kg} \qquad (6)$$

Where V_T = total volume of impeller

Also ρ_i = density of impeller material (stainless AISI 304)

Density of stainless steel (AISI 304) = 800 kg/m^3 [Aerospace Specification Metal ASM Inc]

The length of each rod is 110 mm with each side of the regular hexagon measuring 13 mm.

The sketch and dimensions of the rods are shown below.

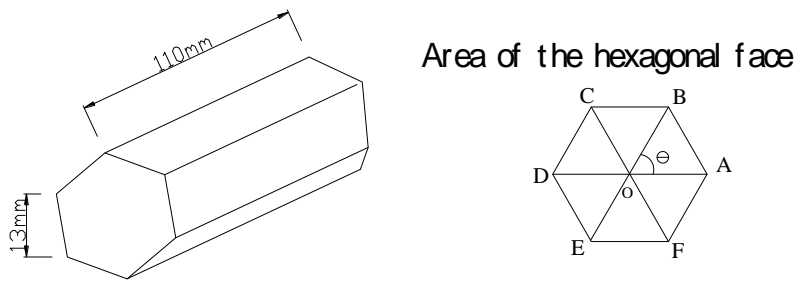


Fig 4: Sketch dimensions of rod

2.2.2 Area of Hexagonal Face (A_h):

$$A_h = [6(\frac{1}{2}a_1 b_1 \sin\theta)] = 0.0008822 \text{ m}^2$$

2.2.3 Volume of 32 Rods (V₃₂):

$$V_{32} = [32(\text{area} \times \text{length})] = 0.00311 \text{ m}^3$$

2.2.4 Volume of Circular Disc (V_{cc}):

$$V_{cc} = \pi r^2 h = 0.00342 \text{ m}^3$$

Where diameter of disc = 330mm and height (L) = 4 mm

2.2.5 Total Volume of Impeller (V_T):

$$V_T = \text{volume of rods} + \text{volume of disc} = 0.003452 \text{ m}^3 \tag{7}$$

2.2.6 Mass of Impeller (M_i):

$$M_i = V_T \times \rho_i = 28 \text{ kg}$$

2.2.7 Force due to Mass of the Impeller (F_i):

$$F_i = M_i g = 280 \text{ N} \tag{8}$$

Where g = acceleration due to gravity = 10 m/sec²

Mass due to the material loaded into the micronizing chamber (M_m). Materials are loaded into the chamber of the micronizer at the rate of 2 kg per minute. M_m = 2 kg

2.2.8 Force due to the Material loaded (F_m):

$$F_m = M_m \times g = 20 \text{ N}$$

The total force F_T due to impeller and material loaded into the machine is

$$F_T = F_i + F_m = 300 \text{ N}$$

2.2.9 Diameters of Pulley Used (Driver and Driven):

The highest speed given to the machine is 3750 rpm with a driven pulley of 100 mm diameter. The electric motor has an output speed of 2900 rpm.

2.2.10 Length Of Belt Connecting The Electric Motor And Micronizing Impeller (L_{b1}):

$$L_{b1} = \frac{\pi}{2}(D_1 + D_2) + \frac{(D_1 - D_2)^2}{4C_d} + 2 C_d = 1\text{m} = 41''$$

2.3 Forces acting on the micronizing impeller shaft:

The schematic representation of the impeller shaft with forces acting on it is shown in Fig 5

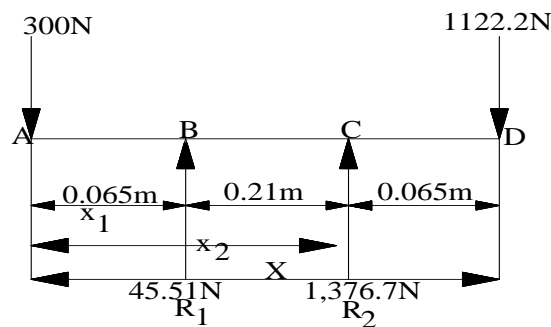


Fig 5: All forces acting on the shaft

The maximum bending moment on the shaft occurred at point C with value of 72.943Nm

2.3.1 Allowable Shear Stress (τ_d):

The stainless steel material AISI 304 as specified by AISI code for allowable shear stress has;

$(\tau_d) = 0.3\sigma_y$ where, $\sigma_y = 215 \times 10^6 \text{N/m}^2$

The presence of key sit on the shaft reduces the value of allowable shear stress (τ_d) by 25%

$\tau_d = 48,375,000 \text{ N/m}^2$

2.3.2 Torque Transmitted (T):

$T = F_c \times r = 56.11 \text{ N}$ (9)

The diameter of the micronizing impeller shaft is thus calculated with ASME code equation

$$D_{si} = \frac{5.1}{\tau_d} \{[(C_m \times M_{max})^2 + (C_t \times T)^2]^{\frac{1}{2}}\}^{\frac{1}{3}}$$

$D_{si} = 30 \text{ mm}$

2.4 Design of Centrifugal Blower:

For a given set of air flow rate and static pressure, the impeller diameter and width of the blower may be calculated from the equation below. Sahay and Singy (1994) gives the equations for calculating the blower parameters as

1. $N_s = \frac{N\sqrt{Q}}{P_s^{0.75}} \text{ rpm}$ (10)

Where N_s = specific speed

N = speed of motor = 3750 rpm

Q = discharge from blower = $10.80 \text{ m}^3 = 384.2 \text{ cfm}$

P_s = static pressure, inches water gauge

$\therefore N_s = 25972$

2. $\phi = \frac{2.35 \times 10^8 P_s}{N^2 d^2}$ (11)

Where ϕ = pressure coefficient = 0.75

d = diameter of impeller (inch) = $9.44'' = 240 \text{ mm}$

3. $w = \frac{175 Q}{\phi N d^2}$ (12)

Where ϕ = flow coefficient = 0.3

W = width of impeller = $1'' = 25.2 \text{ mm}$

4. $\alpha_h = 12 \left(\frac{H_m}{d} - 1\right)$ (13)

Where α_h = blower diffuse angle

H_m = maximum height of blower housing = $440 \text{ mm} = 17.3''$

Or $\alpha_w = 12 \left(\frac{W_m}{d} - 1\right)$ (14)

Where W_m = maximum width of blower. α_w = diffuser angle = 10°

The blower housing width M is calculated as $M = 1.25w + 0.1d = 2.194'' = 55.73 \text{ mm}$

2.4.1 Blower blade design:

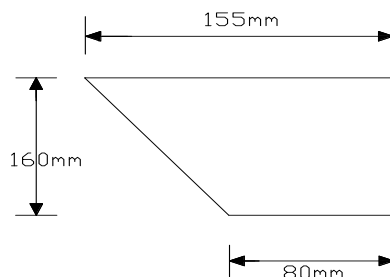


Fig 6: Dimensions of single blade of blower impeller.

The sketch in Fig 6 above shows a single blade of the blower impeller. It has eight (8) trapezoidal blades fixed equidistantly on the face of a circular plate.

The thickness of the stainless steel material plate used is 2mm

2.4.2 Volume of eight (8) Blades (V_b):

$V_b = 8(A_{bb} \times t_{bb}) = 0.000301 \text{ m}^3$

2.4.3 Volume of Circular Disc Carrying the Blades (V_{cd}):

$V_{cd} = \pi r^2 h = 0.0003054 \text{ m}^3$ Where $h = 3 \text{ mm}$

2.4.4 Total Volume of Blower impeller (V_{Tb}):

$$V_{Tb} = V_g + V_{cd} = 0.0006064 \text{ m}^3 \tag{15}$$

2.4.6 Mass of Blower Impeller (M_{bi}):

$$M_{bi} = V_{Tb} \times \rho_i = 4.85 \text{ kg} \tag{16}$$

2.4.7 Force Due to Blower Impeller (F_{bi}):

$$F_{bi} = M_{bi} \times g = 48.5 \text{ N}$$

Torque transmitted is same as micronizing shaft. $T = 56.11 \text{ Nm}$.

The schematic representation of blower impeller shaft with forces acting on it is shown in Fig 7.

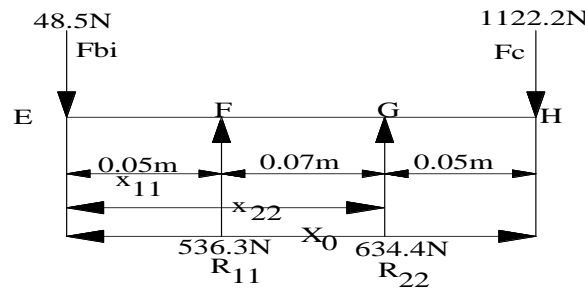


Fig 7: Forces acting on blower shaft

The maximum bending moment occurred at point G with a value of 31.721Nm

Applying the maximum bending moment using a factor of safety 1.2 the shaft diameter is calculated to be;

$$D_{s2} = \left[\frac{5.1}{\tau_d} \{ [(C_m \times M_{max})^2 + (C_t \times T)^2]^{\frac{1}{2}} \right]^{\frac{1}{3}}$$

$$D_{s2} = 25\text{mm}$$

Power Requirement for the Micronizer (P_m):

$$P_m = T \times \omega \tag{17}$$

$$P_m = 56.11 \times 392.73 = 22,037 \text{ W}$$

$$P_m = 22037 \text{ W} = 22 \text{ KW}$$

III MATERIALS AND METHODS:

The soya bean samples used for the study were “Mangu” species from Jos, Plateau State Nigeria obtained at the Main market in Enugu North LGA of Enugu State Nigeria. They were stored in sack bags at stable storage moisture content.

The experimental methods for the soya bean flour production consist of:

- i. Determination of some of the physical parameters of soya bean such as bulk density and moisture content.
- ii. Toasting of soya bean at a temperature of about 90°C
- iii. The reduction of the toasted soya bean to dust (flour) using the micronizer.

3.1 Bulk Density:

The bulk density determination was carried out at Standards Organization of Nigeria (SON) laboratories Enugu. The method used was the standard ratio method of bulk weight to the bulk volume of same material given by the equation;

$$D_b = \frac{M_b}{V_b} = 707.08 \text{ kg/m}^3 \tag{18}$$

Where D_b = bulk density, M_b = Mass of sample, V_b = volume of container used

The weights were determined using electronic (digital) weighing balance [Sportorius Basic: BA 3105].

3.2 Moisture Content Determination:

The moisture content of the samples was determined using the hot air oven method (AOAC, 2002). About 45- 47g for whole grains and 30g for ground samples were placed in containers of known weight and dried in an oven at 105°C to constant weight. The moisture content in percentage (%) dry basis was found by applying the following equation similar to that reported by Bup et al 2008.

$$M_c (\%db) = \left(\frac{M_i - M_f}{M_f} \right) \times 100\% \tag{19}$$

Where M_c is the Moisture content in dry basis, M_i is the initial mass of sample and container (g), M_f is the final mass of sample and container (g) at constant weight. Samples of 9.05% db moisture content were used in the study.

2kg of the prepared samples were fed into the micronizer at different speeds ranging from 1500 rpm – 3750 rpm for each test run of 4 minutes. The micronized materials were then collected using a cyclone. A flexible hose was connected to blower suction outlet and cyclone inlet. The collected material were weighed and tabulated in Table 1.

IV RESULTS AND ANALYSIS:

Table 1: Mass of micronized particles collected at different speeds

S/no	Speed (rpm)	Mass of crushed particle collected(kg)
1	1500	1.41
2	1750	1.56
3	2000	1.80
4	2250	1.85
5	2500	1.88
6	2750	1.84
7	3000	1.76
8	3250	1.68
9	3500	1.55
10	3750	1.28

The analyses of the particles collected from micronizer were carried out at the Department of Pharmaceutics, University of Nigeria Nsukka with an Ocular micro-meter (Karl Kaps; Nr: 39773). The ranges of micron particles in each collection are shown in the tables below. The micrographs of the particles are also shown below.

It was observed that particle sizes above $60\mu\text{m}$ had percentage collection of 58% and 52% for speeds of 1500 and 1750 rpm respectively, implying high coarse particle collection. However, the micrographs show a few “dark spots” indicating lesser fine particle collection as the “dark spots” were formed by fungal growth as a result of agglomeration of particles and biological activity of the samples at the stated moisture content.

Table 2: Data for 1500 rpm speed.

Part Size Range	Freq	% Collection
0.1 - 20	4	8
20.1 - 40	7	14
40.1 - 60	10	20
60.1 - 80	14	28
80.1 - 100	15	30



Fig 8: Micrograph for 1500 rpm sample

Table 3: Data for 1750 rpm speed.

Part Size Range	Freq	% Collection
0.1 - 20	5	10
20.1 - 40	8	16
40.1 - 60	11	22
60.1 - 80	12	24
80.1 - 100	14	28

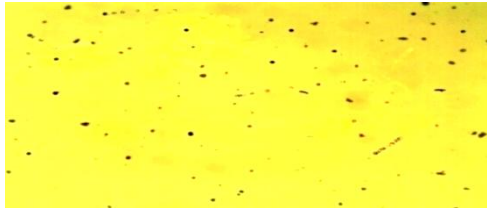


Fig 9: Micrograph for 1750 rpm sample

Table 4: Data for 2000 rpm speed.

Part Size Range	Freq	% Collection
0.1 - 20	7	14
20.1 - 40	9	18
40.1 - 60	13	26
60.1 - 80	13	26
80.1 - 100	8	16



Fig 10: Micrograph for 2000 rpm sample

Table 5: Data for 2250 rpm speed.

Part Size Range	Freq	% Collection
0.1 - 20	10	20
20.1 - 40	11	22
40.1 - 60	14	28
60.1 - 80	10	20
80.1 - 100	6	12

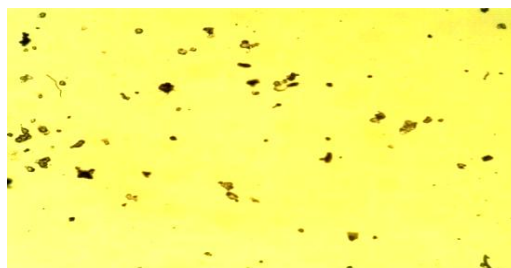


Fig 11: Micrograph for 2250 rpm sample

Table 6: Data for 2500 rpm speed.

Part Size Range	Freq	% Collection
0.1 - 20	15	30
20.1 - 40	16	32
40.1 - 60	14	28
60.1 - 80	5	14
80.1 - 100	0	0



Fig 12: Micrograph for 2500 rpm sample

Speeds of 2000 to 2500rpm showed a shift in trend with more fine particles collected (58, 70 and 90% respectively). This is also shown in the micrographs as there are more “dark spots” as the speeds increased indicating more agglomeration and fungal growth.

Table 7: Data for 2750 rpm speed.

Part Size Range	Freq	% Collection
0.1 - 20	17	34
20.1 - 40	15	30
40.1 - 60	12	24
60.1 - 80	5	10
80.1 - 100	1	2



Fig 13: Micrograph for 2750 rpm sample

Table 8: Data for 3000 rpm speed.

Part Size Range	Freq	% Collection
0.1 - 20	18	36
20.1 - 40	16	32
40.1 - 60	10	20
60.1 - 80	4	8
80.1 - 100	2	4

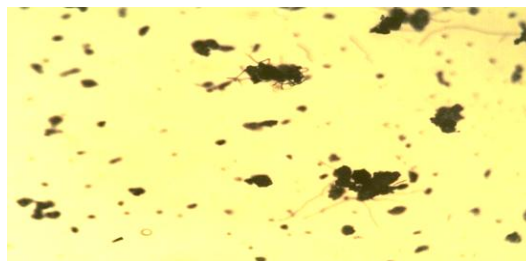


Fig 14: Micrograph for 3000 rpm sample

Table 9: Data for 3250 rpm speed.

Part Size Range	Freq	% Collection
0.1 - 20	17	34
20.1 - 40	15	30
40.1 - 60	10	20
60.1 - 80	4	8
80.1 - 100	4	8



Fig 15: Micrograph for 3250 rpm sample

The trend of finer particle collection continued for speeds of 2750, 3000 and 3250 rpm. This shows that as speeds increased, better size reduction was achieved in the micronizer and finer particles delivered to the cyclone for collection.

Table 10: Data for 3500 rpm speed.

Part Size Range	Freq	% Collection
0.1 - 20	16	32
20.1 - 40	14	28
40.1 - 60	12	24
60.1 - 80	5	10
80.1 - 100	3	6

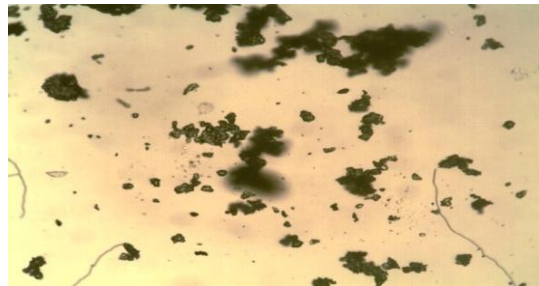


Fig 16: Micrograph for 3500 rpm sample

Table 11: Data for 3750 rpm speed.

Part Size Range	Freq	% Collection
0.1 - 20	17	34
20.1 - 40	13	26
40.1 - 60	10	20
60.1 - 80	6	12
80.1 - 100	4	8



Fig 17: Micrograph for 3750 rpm sample

The particle sizes count obtained using the Ocular micrometer was sorted according to different particle size ranges ({1}0.1- 20, {2} 20.1 – 40, {3} 40.1 – 60, {4} 60.1 – 80 and {5} 80.1 – 100 microns; see Tables 2 to 11) and the percentage collection with respect to speed determined. The cumulative percentage collected for particle size within the range of 0.1 to 60 microns were 42, 48, 58, 70, 90, 88, 88, 84, 70 and 78% respectively for all the speeds in increasing order of magnitude. This shows that speed of 2500 rpm had the best cumulative collection percentage (90%) for the particle size range (between 0.1 and 60 microns) corresponding to flour particles

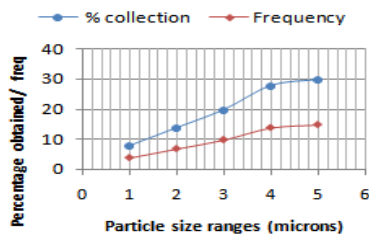


Fig 18: Percentage particle count (1500rpm)

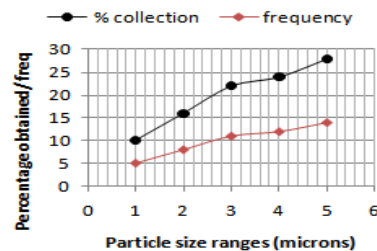


Fig 19: Percentage particle count (1750rpm)

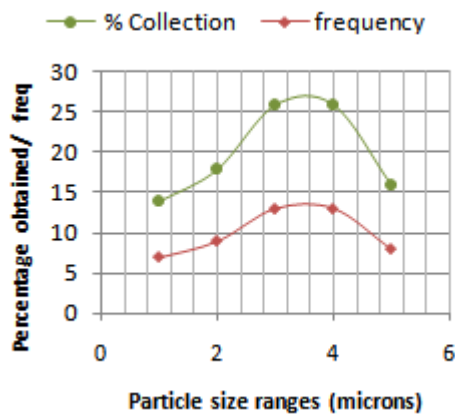


Fig 20: Percentage particle count (2000rpm)

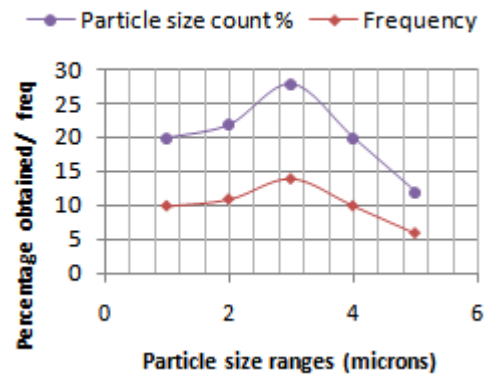


Fig 21: Percentage particle count (2250rpm)

The graphs above give a representation of values obtained in Tables 2 and 3 showing high percentage of coarse particles collection in fig 18 and 19 respectively. The trend changed slightly for speeds of 2000 and 2250 rpm as shown in Fig 20&21. Here there seemed to be equal amounts of very fine and very coarse particles though in smaller quantities hence the plots having a binomial looking curves.

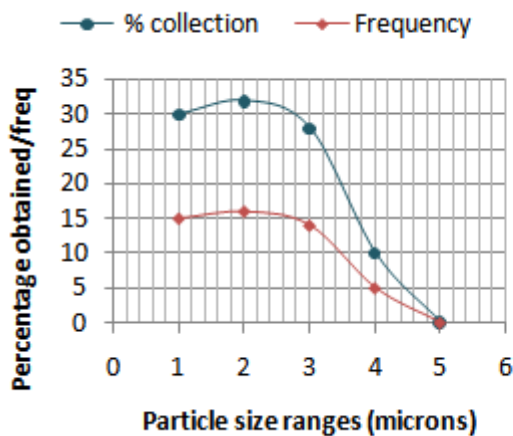


Fig 22: Percentage particle count (2500rpm)

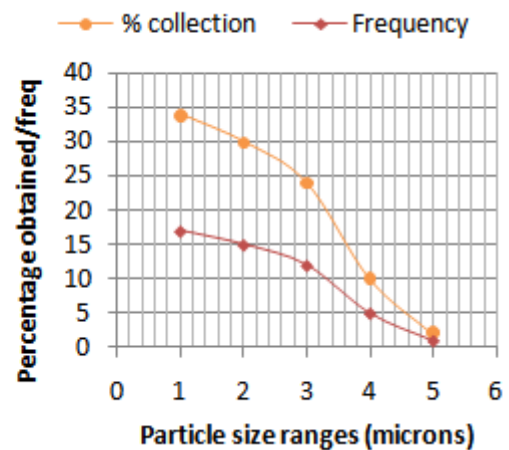


Fig 23: Percentage particle count (2750rpm)

Fig 22 – 25 showed similar trends as the quantities of flour particles increase with attendant decrease in coarse particles. The plots for speeds 3500 and 3750 did not follow any particular trend as shown in fig 26 & 27

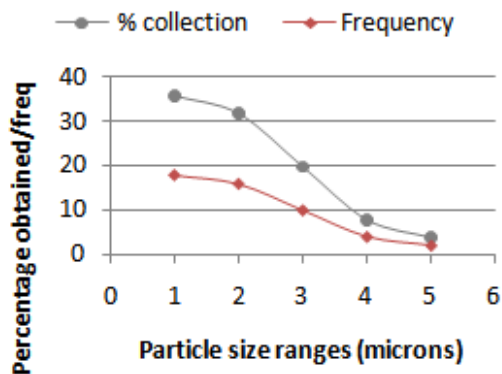


Fig 24: Percentage particle count (3000rpm)

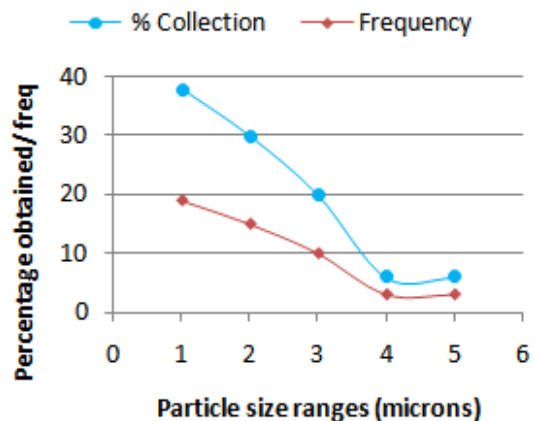


Fig 25: Percentage particle count (3250rpm)

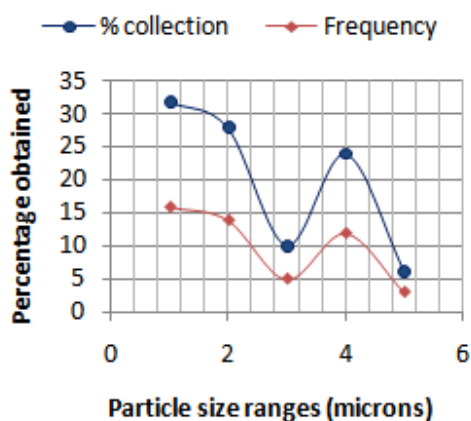


Fig 26: Percentage particle count (3500rpm)

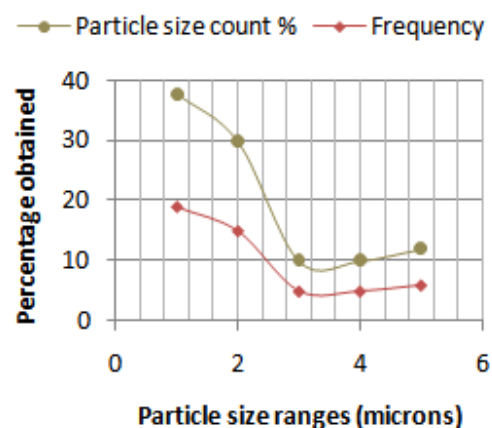


Fig 27: Percentage particle count (3750rpm)

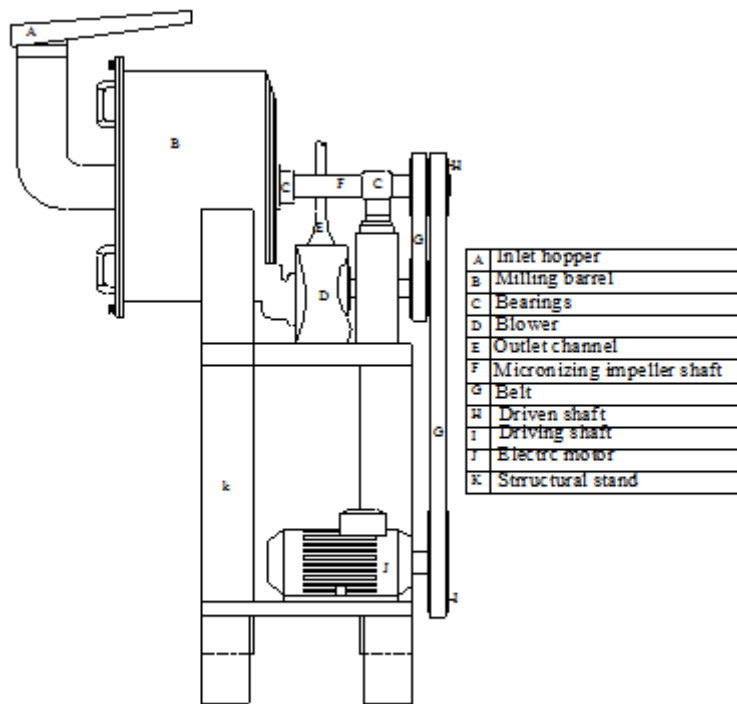
V CONCLUSION:

From the results and analysis carried out above, it can be concluded that the designed micronizer is an effective size reduction machine. It is flexible as it allows for speed control which gives a wider range of crushed material. Particle collection is best achieved with the use of a cyclone. For experimental purposes 2kg was crushed in 4 minutes; however the machine can handle larger quantities of dry material with controlled feed rate. Particle size reduction is commonly used to improve material properties, including more desirable particle size distribution and increased surface area- resulting in better particle flowability, reactivity drying. Bulk density and compatibility (Fitzmill, 2018). Thus, it is expected that the machine would effectively serve small scale industries (flour, fish/poultry feed, pharmaceutical and chemical industries) and would be cost effective.

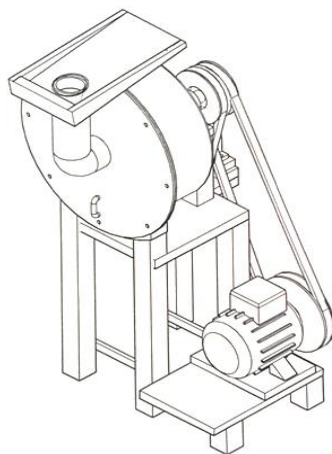
REFERENCES

- [1]. Allen T (1981). "Particle Size Measurement". Chapman & Hills publishers, 3rd Edition. AOAC, (2002). Official Methods of Analysis, 17th Ed. Association of Official Analytical Chemists, Gaithersburg, Maryland, USA.
- [2]. Bup N.D, C'esar K, Dzudie.T, Kuitche A, Abi C.F, and Tchi'egang C., (2008). Variation of the Physical Properties of Sheanut (*Vitellaria Paradoxa* Gaertn.) Kernels during Convective Drying. Intl Journal of Food = Engineering. Volume 4, Issue 7 Article 7
- [3]. Chawla K.K (1998): "Composite Materials"; Science and Engineering: Springer Verlag Berlin 2nd Edition; 403pp
- [4]. Coulson J.M, J.F. Richardson, J.R. Backhurst, and J.H. Harker (1978). Chemical Engineering Unit Operations: Volume Two, Third Edition (S.I.Units) Pergamus Press. Fitzmill (2018). "Particle Size Reduction". www.fitzmill.com/technology/size-reduction
- [5]. Ghaid J.S.A, Robert G. G and Michael J. G (2009). " Effect of particle size on kinetics of starch digestion in milled barley and sorghum grain by porcine alpha-amylase". Journal of Cereal Science 50 (2), pp. 198-204.
- [6]. Gregory R. Z and Richard H (2017). " Particle Size Reduction". Beckett's Industrial Chocolate Manufacture and Use. pp. 216-240.
- [7]. Marianne E. W and Thomas F. J (2002). "The Effect of particle Size Reduction by Grinding on Subsampling Variance for Explosives Residues in Soil". Chemosphere, Vol 49, Issue 10, pp. 1267-1273 Menardo S and Balsari P (2012). " The Effect of Particle size and thermal pre-treatment on the methane yield of four agricultural by-Products." Bioresource Technology, Vol 14, pp. 708-714
- [8]. Pallmann, H., 2011. What you should know before selecting size reduction machines. Pallman Industries inc. CSC Publishing, Powder and Bulk Engineering. Atlantic Way, NJ: United States. Sahay, K.M and Singy, K.K (1994). Unit operations of agricultural processing: First edition
- [9]. Scott W, T. Kendrick, J. Tomaka, and J. Cain (2002). Size reduction solutions for hard-to-reduce materials. Powder and Bulk Engineering. The Fitzpatrick Co. 832 Industrial Drive Elmhurst, IL. www.fitzpatrick.be
- [10]. Fitzmill (2018). "Particle Size Reduction". www.fitzmill.com/technology/size-reduction

APPENDIX I



SIDE VIEW OF MICRONIZER



ISOMETRIC VIEW OF MICRONIZER

Oriaku E. C. "Design and Performance Evaluation of a Dry Grain Microniser" American Journal of Engineering Research (AJER), vol. 7, no. 5, 2018, pp.316-328.